

Properties of Metallic Nanowires: From Conductance Quantization to Localization

J. I. Pascual, J. Méndez, J. Gómez-Herrero, A. M. Baró, N. Garcia, Uzi Landman,* W. D. Luedtke, E. N. Bogachek, H.-P. Cheng

Material structures of reduced dimensions exhibit electrical and mechanical properties different from those in the bulk. Measurements of room-temperature electronic transport in pulled metallic nanowires are presented, demonstrating that the conductance characteristics depend on the length, lateral dimensions, state and degree of disorder, and elongation mechanism of the wire. Conductance during the elongation of short wires (length $\ell \sim 50$ angstroms) exhibits periodic quantization steps with characteristic dips, correlating with the order-disorder states of layers of atoms in the wire predicted by molecular dynamics simulations. The resistance R of wires as long as $\ell \sim 400$ angstroms exhibits localization characteristics with $\ln R(\ell) \sim \ell^2$.

Material systems of reduced size or dimensionality may, and often do, exhibit properties different from those found in the bulk. These include quantized conductance (1, 2) in point contacts and narrow channels whose characteristic (transverse) dimensions approach the electronic wavelength, localization phenomena in low-dimensional systems (3), and mechanical properties characterized by a reduced propensity for the creation and propagation of dislocations in small metallic samples (4–7). Such phenomena are of considerable scientific and technological interest, particularly in the area of miniaturized, highly compact, electronic devices.

Most studies of electronic transport phenomena in microconstrictions are currently performed on high-purity two-dimensional (2D) electron-gas systems having a large Fermi wavelength ($\lambda_F \approx 400$ Å) and are conducted under cryogenic conditions (2). In contrast, our focus here is on room-temperature transport in 3D metallic nanowires with $\lambda_F \approx 5$ Å. In such systems, where the width of the constriction is of the order of λ_F , the atomic-scale structure, imperfections, impurities, and diffusive boundary scattering are expected to play an important role. Nevertheless, room-temperature measurements (8) made with a scanning tunneling microscope (STM) have shown that short and thin Au nanowires (~ 40 Å long) exhibit conductance quantization (1, 2, 9–15), attributed to changes in the contact area during elongation of the

wire and to a decrease in the number of transverse modes or channels in the stretched junction. Such quantized conductance steps have also been observed in other measurements (16–18), as well as the formation of long Pb wires at elevated temperatures (19).

In this report we investigate the evolution of room-temperature electronic transport properties in Au nanowires, from quantized conductance [in $2e^2/h$ or $2(2e^2/h)$ steps, where h is Planck's constant] with a spatial periodicity of ~ 2 Å during elongation of short (~ 50 Å) wires, to the onset of localization in long (100 Å $< \ell < 400$ Å) ones. Combining electronic conductance measurements with molecular dynamics (MD) simulations of the wire elongation process reveals that for short wires, the periodic occurrence of quantized conductance, accompanied by characteristic “dips”

[local conductance minima associated with the presence of disorder (20)], is correlated with atomic-scale structural transformations that occur during the layer-by-layer order-disorder elongation process. The dominance of disorder and the onset of localization in long wires (longer than the localization length) are shown by a nonlinear dependence of the resistance R on the length of the wire ℓ as it is pulled continuously [that is, $\ln R(\ell) \sim \ell^2$]. Moreover, current versus voltage data, recorded at selected stages in the elongation process, indicate gradual loss of metallic character as the long wire narrows.

In our experiments, contact between the tip and the substrate is produced either by the application of a voltage pulse or by indentation, starting from typical STM tunnel conditions. Once the contact is produced, as indicated by the electrical current flowing between the two electrodes, we elongate the contact by retracting the tip slowly (~ 1 Å/s). To achieve optimal control over the STM operations, we have developed a digital control unit (21) that allows us to break the feedback loop at any prescribed time and act on the piezo element (z -piezo) that controls the relative displacement in the z direction between the tip assembly and the substrate. We carried out experiments at room temperature, using homemade STM heads operating either under ambient conditions or at ultrahigh vacuum (UHV). Gold evaporated onto mica and Au(110) single crystals were used as samples, and Pt-Ir and Au tips were used interchangeably [our results are insensitive to the kind of tip used; most likely, the Pt-Ir tip apex is covered with Au atoms once the tip touches the sample (5–7)]. Because the wires are more easily formed in air, the data

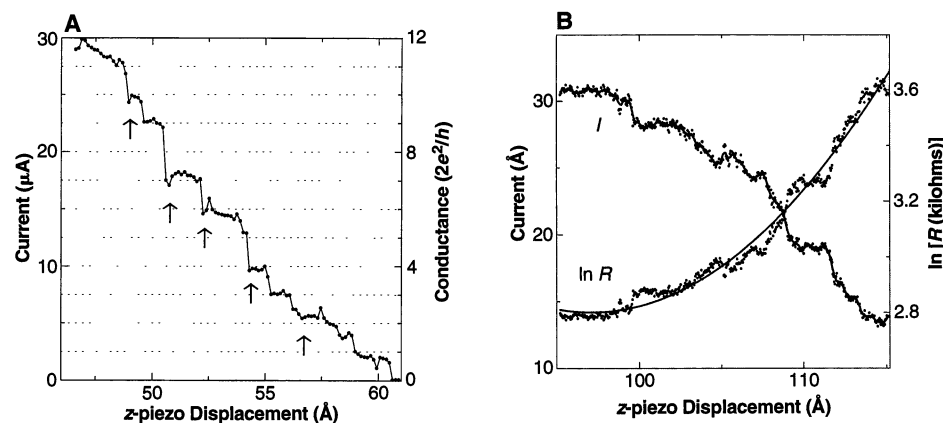


Fig. 1. (A) Current and conductance in a short wire (~ 50 Å) during elongation; this process exhibits room-temperature conductance quantization steps. Dashed lines denote $2e^2/h$ intervals. Arrows indicate dips, associated with disordered elongation stages, which become somewhat less pronounced toward the breaking of the wire. (B) Left scale: Current in a 95 Å wire as it is pulled 20 Å more, to the breaking point. A voltage of 500 mV was applied in the measurement. The smoothed line is introduced for clarity. Right scale: natural logarithm of the resistance of the wire during the elongation process. The solid line corresponds to $\ln R = a + b(z - z_0)^2$ with $a = 2.8$, $b = 2.6 \times 10^{-3}$, and $z_0 = 97$ Å.

J. I. Pascual, J. Méndez, J. Gómez-Herrero, A. M. Baró, Departamento de Física de la Materia Condensada, Universidad Autónoma de Madrid, E-28049 Madrid, Spain. N. Garcia, Física de Sistemas Pequeños, Consejo Superior de Investigaciones Científicas, Universidad Autónoma de Madrid, E-28049 Madrid, Spain. U. Landman, W. D. Luedtke, E. N. Bogachek, H.-P. Cheng, School of Physics, Georgia Institute of Technology, Atlanta, GA 30332, USA.

*To whom correspondence should be addressed.

presented in this report were measured under ambient conditions. However, similar results were obtained in UHV.

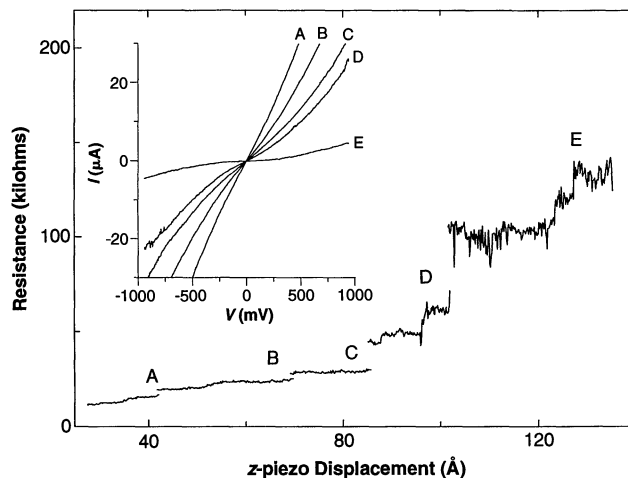
Experiments were performed on a large number of wires (both short and long ones). Typical data are shown in Fig. 1A for the conductance of a short wire ($\sim 50 \text{ \AA}$). We produced these data by bringing a Pt-Ir tip into contact with an Au surface at room temperature and subsequently elongating the contact slowly by retracting the tip (a constant bias voltage of 32 mV was applied during the process). We maintained constant voltage during the measurements by using a low-gain current-voltage (I - V) converter as explained in (8). The conductance exhibits quantized steps in one or two units of $2e^2/h$, and the elongation interval between successive steps either is $\sim 2 \text{ \AA}$ or is split into two intervals whose combined length is $\sim 2 \text{ \AA}$. Furthermore, minima (dips) tend to accompany the quantized jumps (see below).

Next we present data for a long wire that was produced by the elongation of the contact for 95 \AA under a constant bias voltage of 500 mV [a deeper indentation of the tip into the substrate before elongation of the contact generates larger contacts and results in longer pulled wires (5–7)]. At this point, the long wire, having a contact resistance of 15 kilohms, was pulled further for an additional 20 \AA until it broke (Fig. 1B). High values of the contact resistance were reached, which in the case of the data shown in Fig. 1B increases from ~ 16 to 37 kilohms. These values are considerably higher than 12.9 kilohms, the resistance of one quantum conductance channel. For the data shown in Fig. 2, where a resistance as high as 150 kilohms was reached, a Pt-Ir tip was retracted for 185 \AA before breaking occurred, during the application of a bias voltage of 100 mV. In this experiment we stopped the elongation process at five different values of the wire resistance to perform fast ($\sim 0.1 \text{ s}$) measurements of I - V characteristics (inset, Fig. 2).

The observed voltage dependence of the current through the wire (Fig. 2) indicates a transition from a metallic, linear character for long wires with a large cross-sectional area (lower resistance) to a semiconducting or insulating-like regime for longer and narrower wires. Although further studies of this behavior are necessary, it is suggested (15) that these observations may be a consequence of increasing disorder in the wire or may imply Coulomb charging or the increasing importance of electron-electron correlations as such long wires become thinner, possibly leading to the appearance of conductivity gaps.

To discuss the origins of these experimental results, we correlate them with extensive MD simulations, where retraction of

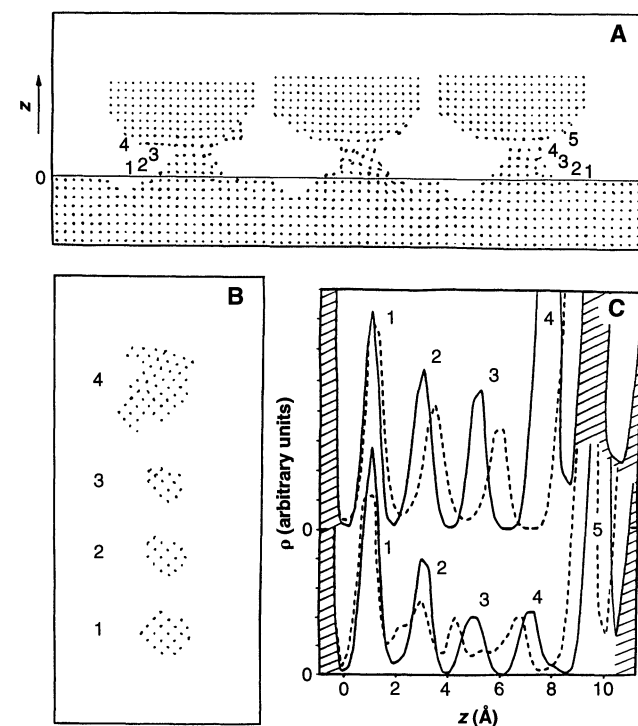
Fig. 2. Resistance versus elongation of a wire that was pulled up to 185 \AA in total. Elongation was stopped at five places (A through E) to measure the I - V spectra shown in the inset. We conducted the retraction at a constant speed of the order of 1 \AA s^{-1} while applying a constant voltage of 100 mV. Letters indicate the stopping points at which the I - V data were acquired (ten such measurements were made at each point). The discontinuities after I - V measurements may be due to some changes in the wire during the experiment.



a tip from an Au surface after contact resulted in the formation of a solid Au junction (5–7). The elongation of the junction in response to the applied external pulling force at room temperature, simulated by means of an overall slow translation of the tip to allow for dynamical structural relaxations, consists of a sequence of stepwise elongation stages, which were predicted (5–7) to result in oscillations, with approximate interlayer distance periodicity, in the recorded force. In each elongation stage, atoms in layers (mainly in the vicinity of the narrowest part of the junction) respond first by accumulations of stress accompanied by strained configurations of the wire

(which remains ordered in atomic layers, although with increasing nonuniformity of the interlayer spacings). This stage is followed by a shorter period of atomic disordering and rearrangement that culminates in the formation of an added layer, with a relief of the accumulated stress and restoration of a higher degree of order in the wire. Consequently, each such elongation-necking stage results in a more extended crystalline junction (in increments of the order of the interlayer spacing in the junction, that is, $\sim 2 \text{ \AA}$) of a smaller cross-sectional neck area (see Fig. 3, A and B). Details of the elongation mechanism may depend on the dimensions (length and width) of the wire

Fig. 3. (A) Side views of atomic configurations obtained from short-time trajectories during a MD simulation (5) of a Ni tip slightly indented into, and then retracted from, an Au(001) surface at 300 K. On the left, a four-layer ordered Au junction formed between the tip and the substrate (the fourth layer of the junction coats the bottom of the tip); the middle configuration demonstrates disorder in the junction during elongation, culminating in the five-layer ordered junction shown on the right. (B) Top views of the in-layer atomic arrangements corresponding to the four-layer ordered wire. (C) Profiles of atomic densities plotted versus distance (z) along the axis of the wire. The solid lines in the upper and lower parts of the figure correspond to the four-layer and five-layer ordered junctions, respectively [left and right configurations in (A)]. The dashed line in the upper part corresponds to the four-layer strained configuration, and the dashed line in the lower part to the disordered structure [middle configuration in (A)] that developed during the elongation process. Hatched regions represent Au substrate ($z \leq 0$) and Ni tip layers.



as well as on the structure, composition, and crystalline orientation of the surface, wire, and tip, which can influence the modes of plastic yielding and reordering processes. For example, in the aforementioned simulations involving a Ni tip, an Au(001) surface, and a small-radius connective junction (wire), the elongation process did not appear to involve slip along well-defined glide planes. However, in room-temperature elongation simulations (7) of a larger (75 Å long) Au(111) wire, tapered to an initial midneck radius of ~17 Å, we observed, at various stages, slip events that may occur along a system of glide planes [for example, (111) and (110)] and more localized (not involving slip) disordering-ordering layer-addition processes that become dominant for smaller cross sections. Indeed, although we focus here on measurements of conductance quantization in thin wires (characterized by about 10 or less conductance channels), our experiments on thicker wires show a different pattern (less well-defined plateaus and steps and variable conductance step heights), transforming to the behavior shown in Fig. 1A as the wire narrows.

To illustrate the elongation process, we show in Fig. 3A side views of atomic configurations, starting from a layer-ordered junction containing four atomic layers (see the corresponding intralayer atomic arrangements shown in Fig. 3B) and ending with a longer layer-ordered junction containing five layers, along with a structure during the intervening disordered stage. Corresponding plots of the atomic density profiles along the normal axis (z) of the junction shown in Fig. 3C illustrate the atomic distributions in the initial and final ordered stages of the junction and during the straining and disordering stages of the transformation.

During elongation, the wire evolves through atomic configurations with various degrees of order and disorder. Even in the ordered stages, which exhibit crystalline-like atomic layers along the axis of the junction, the shapes of the layers are rather irregular (see Fig. 3B), resulting in a solid wire with a surface roughness of a few angstroms, comparable to the wavelength of the electron (~4 Å). Although such an aspect of disorder may not greatly affect the mechanical characteristics, it can influence electronic transport processes.

The appearance of room-temperature quantized conductance in the short wires and its persistence [see Fig. 1A, where nine steps of height $G_0 = 2e^2/h$ or $2(2e^2/h)$, with a period $d \sim 2$ Å, the interlayer spacing in the material, are seen] are quite remarkable, particularly in view of the known sensitivity of conductance quantization to the presence of disorder (which in our wires includes

surface roughness and disorder occurring between the intermittent layer-ordered stages) (see Fig. 3). This result implies that, overall, wires in this length regime maintain a sufficient degree of crystalline order (Fig. 3) to sustain quantization of the conductance.

Furthermore, significant insights into the microscopic mechanism of the elongation process and the nature of disorder in the wire are provided by the observation of dips that accompany the quantized conductance steps (see Fig. 1A). Such conductance dips have been discussed (20) in the context of static disorder in 2D systems, where their occurrence, for a sufficient degree of disorder, was shown to be accompanied by rounding of the conductance steps and loss of quantization in units of G_0 . In our case, the degree and distribution of disorder in the wire change during the elongation process. Moreover, our data (Fig. 1A) exhibit sharp steps, plateaus, and clear quantization in units of G_0 or $2G_0$. Consequently, although some intrinsic disorder in the wire may contribute to the occurrence of such dips, we associate them mainly with electron scattering caused by the enhanced structural disorder that develops toward the completion of each of the discrete elongation stages of the wire. The rapid rise in the conductance after each dip indicates restoration of a higher degree of order in the pulled wire subsequent to the disordering-rearrangement elongation stage. In addition, the variability in the conductance quantization step height (one or two $2e^2/h$ units) and the occasional occurrence of two successive steps in an elongation interval of combined length $\sim d$ (see Fig. 1A) may originate from stick-slip characteristics of the straining-yielding elongation process and from factors that influence the quantization of transverse electronic states (channels) in the wire (these include accidental degeneracies of transverse electronic modes, irregular layer shapes, and most likely the occurrence of intermediate atomic configurations during the elongation process that satisfy the condition for closing of a conductance channel). These observations support a correlation between the measured patterns and the aforementioned periodic layerwise order-disorder elongation mechanism of the wire.

In contrast, conductance quantization was not observed during elongation of long wires ($\ell \geq 100$ Å, see Fig. 1B). For such long, quasi-1D wires, in which the resistance reaches values much higher than the quantum unit of resistance, one may expect localization signatures (3), if the length of the wire ℓ exceeds the localization length L , implying an exponential growth of the resistance R with ℓ , that is, $R(\ell) \sim \exp(\ell/L)$.

However, because the wire is being continuously pulled, the value of L may vary, depending on the elongation. The localization length is given by (22) $L \sim Sk_F^2\lambda$,

where S is the cross-sectional area of the wire, k_F is the Fermi wave vector, and λ is the elastic mean free path. Because the volume Ω of the wire remains constant during room-temperature elongation [as observed in MD simulations (5–7)], S decreases with increasing ℓ (for a cylindrical wire $S = \Omega/\ell$). Using this relation in $\exp[\ell/L(\ell)]$ leads to a nonlinear dependence, $\ln R(\ell) \sim \ell^2$. Indeed, such a dependence of the measured R on ℓ is depicted in Fig. 1B (values of $L \leq 40$ Å may be estimated from these data).

These observations, which correlate with the wire elongation mechanism predicted by MD simulations, demonstrate the size-evolutionary patterns of properties in material systems of reduced dimensions. Such patterns are of fundamental as well as technological importance, particularly for nanostructured and miniaturized devices.

REFERENCES AND NOTES

1. R. Landauer, *J. Phys. Condens. Matter* **1**, 8099 (1989).
2. C. W. J. Beenakker and H. Van Houten, *Solid State Phys.* **44**, 1 (1991).
3. P. W. Anderson, *Phys. Rev.* **109**, 1492 (1958); see review by P. A. Lee and T. V. Ramakrishnan, *Rev. Mod. Phys.* **57**, 287 (1985).
4. R. W. Siegel, *Mater. Sci. Eng. B* **19**, 37 (1993).
5. U. Landman, W. D. Luedtke, N. A. Burnham, R. J. Colton, *Science* **248**, 454 (1990).
6. U. Landman and W. D. Luedtke, *J. Vac. Sci. Technol.* **9**, 414 (1991).
7. W. D. Luedtke and U. Landman, in preparation.
8. J. I. Pascual *et al.*, *Phys. Rev. Lett.* **71**, 1852 (1993).
9. N. Garcia and L. Escapa, *Appl. Phys. Lett.* **54**, 1418 (1989); N. Garcia, paper presented at the STM Workshop, International Center for Theoretical Physics, Trieste, 1987.
10. L. I. Glazman, G. B. Lesovik, D. E. Khmel'nitskii, R. I. Shekhter, *Pis'ma Zh. Eksp. Teor. Fiz.* **48**, 218 (1988) [*JETP Lett.* **48**, 238 (1988)]; A. Yacoby and Y. Imry, *Phys. Rev. B* **41**, 5341 (1990).
11. S. Ciraci and E. Tekman, *Phys. Rev. Lett.* **62**, 1860 (1989).
12. N. D. Lang, A. Yacoby, Y. Imry, *ibid.* **63**, 1499 (1989).
13. E. N. Bogachev, A. M. Zagorskii, I. O. Kulik, *Fiz. Nizk. Temp.* **16**, 1404 (1990) [*Sov. J. Low. Temp. Phys.* **16**, 796 (1990)]; E. N. Bogachev, M. Jonson, R. I. Shekhter, T. Swahn, *Phys. Rev. B* **47**, 16635 (1993).
14. J. A. Torres, J. I. Pascual, J. J. Saenz, *Phys. Rev. B* **49**, 16581 (1994).
15. M. Ogata and H. Fukuyama, *Phys. Rev. Lett.* **73**, 468 (1994).
16. N. Agrait, J. G. Rodrigo, C. S. Sirvant, S. Vieira, *Phys. Rev. B* **48**, 8499 (1993).
17. L. Olesen *et al.*, *Phys. Rev. Lett.* **72**, 2251 (1994).
18. J. M. Krans *et al.*, *Phys. Rev. B* **48**, 14721 (1993).
19. L. Kuipers and J. W. M. Frenken, *Phys. Rev. Lett.* **70**, 3907 (1993).
20. I. Kander, Y. Imry, U. Sivan, *Phys. Rev. B* **41**, 12941 (1990).
21. J. M. Gomez-Rodriguez *et al.*, in preparation.
22. D. J. Thouless, *Phys. Rev. Lett.* **39**, 1167 (1977).
23. Useful discussions with J. J. Saenz and experimental software support by J. M. Gomez-Rodriguez are acknowledged. The work of J.I.P., J.M., J.G.-H., and A.M.B. was supported by Comision Interministerial de Ciencia y Tecnologia (CICYT) under project PB92-0158. The work of N.G. was supported under CICYT project MAT92-0129 and BRITE contract BRE2-0971. The work of U.L., W.D.L., E.N.B., and H.-P.C. was supported by U.S. Department of Energy grant DE FG05-86ER45234, the Air Force Office of Scientific Research, and the National Science Foundation.

25 October 1994; accepted 2 February 1995